

RESEARCH

Open Access



The impact of culture systems on the gut microbiota and gut metabolome of bighead carp (*Hypophthalmichthys nobilis*)

Chen Ye^{1,2}, Shiyu Geng^{1,2}, Yingyu Zhang^{1,2}, Huimin Qiu^{1,2}, Jie Zhou^{1,2}, Qi Zeng^{1,2}, Yafei Zhao¹, Di Wu^{1,2}, Guilan Yu^{1,2}, Haibo Gong³, Beijuan Hu^{1,2,4*} and Yijiang Hong^{1,2,4*}

Abstract

Background The gut microbiota of fish confers various effects on the host, including health, nutrition, metabolism, feeding behaviour, and immune response. Environment significantly impacts the community structure of fish gut microbiota. However, there is a lack of comprehensive research on the gut microbiota of bighead carp in culture systems. To demonstrate the impact of culture systems on the gut microbiome and metabolome in bighead carp and investigate a potential relationship between fish muscle quality and gut microbiota, we conducted a study using 16S ribosomal ribonucleic acid sequencing, gas chromatography-mass spectrometry, and liquid chromatography-mass spectrometry techniques on bighead carp in three culture systems.

Results Our study revealed significant differences in gut microbial communities and metabolic profiles among the three culture systems. We also observed conspicuous changes in muscle structure. The reservoir had higher gut microbiota diversity indices than the pond and lake. We detected significant differences in phyla and genera, such as Fusobacteria, Firmicutes, and Cyanobacteria at the phylum level, *Clostridium sensu stricto 1*, *Macellibacteroides*, *Blvii28 wastewater sludge group* at the genus level. Multivariate statistical models, including principal component analysis and orthogonal projections to latent structures-discriminant analysis, indicated significant differences in the metabolic profiles. Key metabolites were significantly enriched in metabolic pathways involved in "arginine biosynthesis" and "glycine, serine, and threonine metabolism". Variation partitioning analysis revealed that environmental factors, such as pH, ammonium nitrogen, and dissolved oxygen, were the primary drivers of differences in microbial communities.

Conclusions Our findings demonstrate that the culture system significantly impacted the gut microbiota of bighead carp, resulting in differences in community structure, abundance, and potential metabolic functions, and altered the host's gut metabolism, especially in pathways related to amino acid metabolism. These differences were influenced substantially by environmental factors. Based on our study, we discussed the potential mechanisms by which gut microbes affect muscle quality. Overall, our study contributes to our understanding of the gut microbiota of bighead carp under different culture systems.

Keywords Culture system, Gut microbiota, Metabolome, Bighead carp, Fish muscle quality

*Correspondence:

Beijuan Hu
beijuanhu@ncu.edu.cn
Yijiang Hong
yjhong@ncu.edu.cn

Full list of author information is available at the end of the article



© The Author(s) 2023. **Open Access** This article is licensed under a Creative Commons Attribution 4.0 International License, which permits use, sharing, adaptation, distribution and reproduction in any medium or format, as long as you give appropriate credit to the original author(s) and the source, provide a link to the Creative Commons licence, and indicate if changes were made. The images or other third party material in this article are included in the article's Creative Commons licence, unless indicated otherwise in a credit line to the material. If material is not included in the article's Creative Commons licence and your intended use is not permitted by statutory regulation or exceeds the permitted use, you will need to obtain permission directly from the copyright holder. To view a copy of this licence, visit <http://creativecommons.org/licenses/by/4.0/>.

Background

The gut microbiota in fish has been proven to have significant effects on the health [1, 2], nutrition [3, 4], and metabolism of the host [5, 6].

The fish gut microbiota is shaped by environmental factors, including microbial community structure [7], diversity, and richness [8]. Previous studies have reported significant alterations in the intestinal microbial communities of various fish species due to environmental factors [9–11].

Our previous study [12] showed significant differences in bighead carp muscle fatty acids, amino acids, and volatile flavour compounds in different aquaculture systems, suggesting that the culture systems could affect muscle quality. However, the potential relationship between the culture systems and muscle quality needs further exploration [12], where gut microbes may play a crucial role. Studies have reported the impact of gut microbiota on muscle quality in other species [13, 14]. However, little research has been done to explore the microbiota's role in improving fish muscle quality.

Bighead carp (*Hypophthalmichthys nobilis*), which belongs to the order Cypriniformes, family Cyprinidae, subfamily Hypophthalmichthyinae, and genus *Hypophthalmichthys* [15], is referred to China as one of the "four major domesticated fish" [16]. It is an omnivorous filter-feeding fish [17] that is highly popular in China due to its affordability, delicious taste, and high nutritional value [18]. It is also one of the world's most important aquaculture species [19], with an output of 3.187 million tons, accounting for 6.5% of the world's inland finfish production [20]. Previous studies have mainly focused on the gut microbiota of bighead carp in ponds [21–26], with limited research conducted in lakes [16, 27–30] and reservoirs [28–30]. There is a lack of comprehensive studies on the gut microbiota of bighead carp in conventional culture systems.

Therefore, this study aimed to investigate the impact of three typical culture systems on the gut microbiota, gut metabolome, and muscle structure of bighead carp. In addition, we explored the potential mechanisms by which gut microbes and gut metabolites drive changes in muscle quality in bighead carp.

Methods

Fish, culture systems, and sampling

Two-year-old bighead carp with a body length of 35.0 ± 3.70 cm, body width of 7.8 ± 0.6 cm, and body weight of 1.20 ± 0.10 kg were purchased from the same breeding farm and cultured in the three culture systems in March 2016: NC (Nancheng), which is a culture pond; PY (Poyang), which represents the inner lake of Poyang

Lake, the largest freshwater lake in China; and XHK (Xiahuikeng), which is an alpine cold-water reservoir at 420 m. The water surface areas of NC, PY, and XHK are 0.53, 40, and 90 ha, respectively.

Bighead carp in NC were fed artificially, while fish in PY and XHK were free-range. The biochemical composition of the formulated feed in NC was moisture $\leq 12.0\%$, crude protein $\geq 28.0\%$, crude fibre $\leq 11.6\%$, crude ash $\leq 15.0\%$, crude lipid $\geq 3.5\%$, total phosphorus $\geq 0.7\%$, and lysine $\geq 1.3\%$.

A total of 30 bighead carp representing three groups with ten replicates were randomly caught and anaesthetized with an overdose of tricaine methane sulfonate in March 2017. The hindgut content of bighead carp was extracted under aseptic conditions, washed with phosphate buffer saline, placed in sterile centrifuge tubes, frozen in liquid nitrogen until fully frozen, and then stored at -80 °C for deoxyribonucleic acid (DNA) and metabolite extraction. The white epaxial muscle was cut transversely into 0.5×0.5 cm blocks and fixed in formalin for 24 h.

Environmental factors measurement

During the cultural period, environmental factors of the culture systems were tracked every season. Water temperature (WT), dissolved oxygen (DO), pH, nitrate nitrogen ($\text{NO}_3\text{-N}$), and ammonium nitrogen ($\text{NH}_4\text{-N}$) were measured by YSI Pro Plus multiparameter instrument. Transparency was obtained by measuring the maximum visible depth of the Secchi disk underwater.

Muscle histology

Fixed blocks were embedded in paraffin, sectioned, and stained with hematoxylin and eosin [31]. Tissue images were photographed using a Nikon DS-Ri2 microscope camera. Muscle cells from the image of each sample were segmented with Cellpose 2.0 software [32]. The long and short diameters of muscle fibres were measured with Fiji [33].

DNA extraction, 16S ribosomal ribonucleic acid rRNA (16S rRNA) gene sequencing, and data processing

According to the instruction manual, DNA from intestinal contents was extracted using a DNeasy PowerSoil Kit (QIAGEN, Germany). The concentration and integrity of DNA were measured with a NanoDrop 2000 spectrophotometer (NanoDrop, USA) and agarose gel. The V3–V4 hypervariable region of the bacterial 16S rRNA gene was amplified by polymerase chain reaction (PCR) with universal primer pairs (343F/798R) [34]. The amplicon quality was visualised using gel electrophoresis. The PCR products were purified with Agencourt AMPure XP beads (Beckman Coulter, USA) and quantified using a

Qubit dsDNA assay kit. Sequencing was performed on an Illumina NovaSeq 6000 (Illumina, USA).

The raw image data file was transformed into raw sequence data through base recognition analysis. Paired-end reads were preprocessed using Trimmomatic software [35], which removed ambiguous bases and low-quality sequences with average quality scores below 20 using a sliding window trimming approach. Paired-end reads were then assembled using fast length adjustment of short reads software [36]. Reads with 75% of bases above Q20 were retained, chimaeras were removed, and valid tags were obtained using quantitative insights into microbial ecology (QIIME) software [37]. Clean reads were subjected to primer sequence removal and clustered to generate operational taxonomic units (OTUs) with a 97% similarity cutoff using Vsearch software [38].

All representative reads selected by QIIME were annotated and blasted against the Silva database (v123) [39] using the ribosomal database project naïve Bayesian classifier (confidence threshold: 70%) [40]. The resulting OTU abundance matrix and annotation information were exported for downstream analysis.

In MicrobiomeAnalyst [41], the OTU data were filtered and rarefied to the minimum library size. Bacterial alpha diversity was assessed using the Shannon, Simpson, Chao1, and ACE indices. The distance matrix was calculated using non-metric multidimensional scaling (NMDS) [42] based on Bray-Curtis distance and visualised by the first two coordinates in NMDS. A one-way analysis of similarity (ANOSIM) [43, 44] with 999 permutations was performed to test for the significant difference between groups using the R vegan [45] and ecodist package [46]. Linear discriminant analysis effect size (LEfSe) [47] was applied to identify differences in taxa composition. The taxa with the logarithm to the base 10 of linear discriminant analysis (LDA) score > 2.0 and false discovery rate (FDR) (Kruskal-Wallis test) < 0.05 were regarded as differential taxa. The phylogenetic investigation of communities by reconstruction of unobserved states (PICRUSt2) [48] was applied to predict bacterial function.

Metabolite extraction

40 µL of internal standards (2-chloro-l-phenylalanine in methanol, 0.3 mg/mL, 20 µL; lysophosphatidylcholine 17:0 in methanol, 0.01 mg/mL, 20 µL), 600 µL of extraction solvent with methanol/water (4/1, volume/volume) and steel balls were added to the 60 mg sample. The samples were stored at -20 °C, ground at 60 Hz for 2 min, ultrasonicated for 10 min, held at -20 °C for 30 min, centrifuged at 13,000 rpm, and 4 °C for 10 min. Then, 300 µL of supernatant was collected and dried in a freeze-concentration centrifugal dryer, redissolved in

a 400 µL mixture of methanol and water (1/4, volume/volume), vortexed, ultrasonicated, and centrifuged again. Finally, 150 µL of supernatant was collected via syringes, filtered through 0.22 µm microfilters, and transferred to vials for liquid chromatography-mass spectrometry (LC-MS) analysis.

The 60 mg sample was supplemented with 40 µL of internal standard (2-chloro-l-phenylalanine in methanol, 0.3 mg/mL) and 360 µL of cold methanol. After grinding and ultrasonication at 4 °C for 30 min, 200 µL of chloroform was added to each sample and vortexed at 60 Hz for 2 min. This was followed by the addition of 400 µL of water, another round of vortexing, ultrasonication at 4 °C for 30 min, storage at -20 °C for 30 min, and centrifugation for 10 min. Next, 300 µL of supernatant was transferred to a vial and dried. To the sample, 80 µL of methoxylamine hydrochloride (in pyridine, 15 mg/mL) was added, vortexed for 2 min, and incubated at 37 °C for 90 min. A mixture of 80 µL N, O-Bis(trimethylsilyl)trifluoroacetamide (with 1% trimethylchlorosilane), 20 µL n-hexane and 10 µL fatty acid methyl esters (C8/C9/C10/C12/C14/C16, 0.8 mg/mL; C18/C20/C22/C24/C26, 0.4 mg/mL; all in chloroform) was then added to each sample, vortexed for 2 min and then derivatised at 70 °C for 60 min for gas chromatography-mass spectrometry (GC-MS) analysis.

A quality control (QC) sample was prepared by mixing aliquots of all samples. The QC sample was injected every ten runs for assessment of data repeatability.

LC-MS analysis

The derivatised samples were analysed using a Dionex Ultimate 3000 RS HPLC system equipped with a Q-Exactive quadrupole-Orbitrap mass spectrometer, which had a heated electrospray ionisation source (Thermo Fisher, USA). The ACQUITY UPLC HSS T3 column (1.8 µm, 2.1 × 100 mm, Waters, USA) was used, and the binary gradient elution system consisted of (A) water (containing 0.1% formic acid, volume/volume) and (B) acetonitrile (containing 0.1% formic acid, volume/volume). Separation was achieved using the following parameters: 0–1 min, 5% B; 1–11 min, 5–100% B; 11–13 min, 100% B; 13–13.1 min, 100% to 5% B; 13.1–15 min, 5% B; flow rate, 0.35 mL/min; column temperature, 50 °C; injection volume, 5 µL.

The mass spectrometer was operated as the following parameters: mass range, m/z 70–1000; resolution for the full mass spectrum (MS) scan and MS/MS scans, 70,000 and 17,500, respectively; normalised collision energy and stepped normalised collision energy, 20 eV and 40 eV, respectively; spray voltage, 3800 V (positive) and 3000 V (negative); sheath gas flow rate, 35 arbitrary units; auxiliary gas flow rate, 8 arbitrary units; capillary temperature,

320 °C; Aux gas heater temperature, 350 °C; S-lens RF level, 50 V.

Raw data were collected using UNIFI 1.8.1 software and analysed using Progenesis QI 2.3 software (Waters, USA) with baseline filtering, retention time correction, peak recognition, peak alignment, and integration operations. Isotopic peaks were excluded, and the minimum intensity was set to 15% of the base peak intensity. Metabolites were identified based using the Human Metabolome Database [49], LIPIDMAPS (v2.3) [50], and Metabolite Link [51], based on the exact mass number, secondary mass fragment, and isotope distribution.

Then, the data matrix was outputted with three-dimensional datasets, including m/z , retention time, and peak intensities. The matrix was reduced by removing metabolites with more than 50% missing values, uncertain metabolites, and metabolites with a relative standard deviation (RSD) > 0.4 in QC samples. Then, the remaining missing values were imputed by half of the minimum value. All metabolites were segmented and normalised based on internal standards, and then the internal standards were removed.

GC-MS analysis

The derivatised samples were separated and analysed on an Agilent 7890B gas chromatography system coupled to an Agilent 5977A MSD system with a DB-5MS column (30 m × 0.25 mm × 0.25 µm) (Agilent, USA). The conditions were set as follows: carrier gas, helium; flow rate, 1 mL/min; injector temperature, 260 °C; injection volume, 1 µL by splitless mode. quadrupole temperature, 150 °C; electron impact ion source, 230 °C. The initial oven temperature was 60 °C, ramped to 125 °C at a rate of 8 °C/min, to 210 °C at a rate of 5 °C/min, to 270 °C at a rate of 10 °C/min, to 305 °C at a rate of 20 °C/min, and finally held at 305 °C for 5 min. The ionisation energy was 70 eV. Mass data were acquired in full-scan mode (m/z 50–500), and the solvent delay time was 5 min.

The raw data were converted using Analysis Base File Converter software and processed via Mass Spectrometry-Data Independent Analysis software for peak detection, deconvolution, alignment, and filtering. Metabolites were annotated using a database from Lumingbio company (China). Internal standard ion peaks with RSD > 0.3 were removed, and all peaks were segmented and normalised based on the internal standard and fatty acid methyl esters. All fatty acid methyl esters, internal standards, and known pseudo-positive peaks were then removed. The resulting data matrix was exported, including sample information, peak names, and peak intensities.

Metabolomics analysis

LC-MS and GC-MS data matrixes were combined and imported into Metaboanalyst [52]. The data were transformed and scaled, and then principal component analysis (PCA) and orthogonal projections to latent structures-discriminant analysis (OPLS-DA) [53, 54] were performed. The quality of the OPLS-DA models was evaluated with R^2X and Q^2 . Permutation tests with 1000 permutations were carried out to assess the fitting of the models. Variable importance in projection (VIP) of metabolites was calculated in the OPLS-DA models.

Metabolites with VIP value ≥ 1.0 and p value < 0.05 were considered significantly differential, and those present in all intergroup comparisons were considered key. Metabolic pathway analysis (MetPA) was carried out on these metabolites, and enriched pathways with p value < 0.05 were considered significant.

Association analysis

To investigate potential associations between significant gut microbes and metabolites, we used the R psych package [55]. Spearman rank correlation was applied to filter associated microbes and metabolites with p value < 0.05 and $r > 0.8$.

Variation partitioning analysis (VPA) was performed using the R vegan package to examine the relative importance of environmental factors for gut microbiota variation. Redundancy analysis (RDA) with 999 permutations was carried out to correlate significantly differential microbes at the phylum and genus levels with environmental factors based on the first axis length of detrended correspondence analysis calculated by the R vegan package.

Statistical analysis

Data analysis was performed using R 4.2.0 [56] and SPSS 26.0 (SPSS Inc.). The Wilcoxon test and Kruskal-Wallis test were used for significance testing. Multiple comparisons and the Benjamini-Hochberg method correction were performed when the significance in the Kruskal-Wallis test was less than 0.05. p value or FDR < 0.05 was considered statistically significant. We denoted significance levels with *, **, and *** representing p value or FDR < 0.05, 0.01, and 0.001 between groups, respectively. Values were expressed as mean \pm standard deviation.

Results

Muscle structure

Significant differences were observed in the muscle structure of the three groups of bighead carp. The NC group (Fig. 1A) showed tightly arranged muscle fibres, less connective tissue, and larger myocytes. The PY group

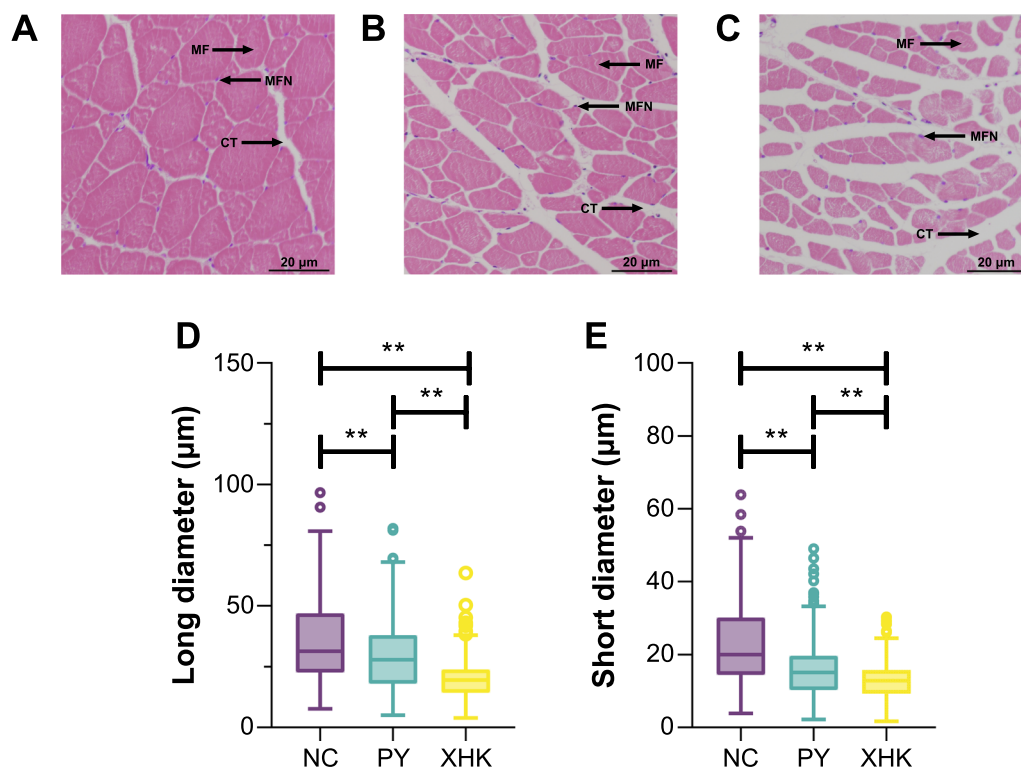


Fig. 1 Transsections of muscle tissues and muscle fibres parameters of bighead carp from three groups. **A** NC $\times 200$; **B** PY $\times 200$; **C** XHK $\times 200$; **D** long diameter of muscle fibres; **E** short diameter of muscle fibres. (MF: muscle fibre; MFN: muscle fibre nucleus; CT: connective tissue). Significance levels with *, **, and *** represent $FDR < 0.05$, 0.01 , and 0.001 between groups, respectively (Kruskal-Wallis test)

(Fig. 1B) and XHK group (Fig. 1C) had loosely aligned muscle fibre, abundant connective tissue, and smaller myocytes.

The long and short diameters of the muscle fibres were also significantly different among all three groups, with NC having the largest, PY the second largest, and XHK the smallest (Kruskal-Wallis, $FDR < 0.05$) (Fig. 1D, E).

Microbial community structure of the gut in bighead carp

The processed data are shown in Additional file 5: Table S1. The microbiota was classified into 19 phyla,

33 classes, 75 orders, 128 families, 172 genera, and 13 species.

At the phylum level (Fig. 2A), the different culture systems had similar community structures but differed in abundance. Proteobacteria and Acidobacteria were significantly higher in PY and XHK than in NC (Kruskal-Wallis test, $FDR < 0.05$), while Fusobacteria, Firmicutes, and Cyanobacteria showed the opposite trend (Kruskal-Wallis test, $FDR < 0.05$). The abundance of Gemmatimonadetes was significantly higher in XHK than in NC (Kruskal-Wallis test, $FDR < 0.05$), and Spirochaetae was significantly higher in PY than in NC

(See figure on next page.)

Fig. 2 The composition, alpha diversity, beta diversity, and indicator of gut microbiota. **A** The composition and relative abundance of the top 10 phyla. The bars with different colours represent different phyla. **B** The composition and relative abundance of the top 10 genera. The bars with different colours represent different genera. **C** The three groups' diversity indices (Shannon, Simpson, Chao1, and ACE). The outliers were calculated by Tukey's test. The horizontal lines of the boxplot, from top to bottom, represent the maximum value except for outliers, upper quartile, median, lower quartile, and minimum value except for outliers, respectively. **D** Every point in the plot represents a sample. NMDS plot shows a clear separation of every two groups. ANOSIM demonstrates that culture systems significantly impacted the gut bacterial community composition ($R > 0$ indicates that the difference between groups is greater than within groups, and $FDR < 0.05$ indicates that the difference is significant). **E, F** LEfSe analysis: The log LDA score of gut microbiota at the phylum and genus levels (log LDA score > 2.0). The bars with different colours represent the significant phyla or genera of the corresponding group. **G** The heatmap of the top 20 significant pathways predicted by PICRUSt2 ($FDR < 0.05$). The boxes with purple colours represent higher expression levels, and yellower colours represent lower expression levels

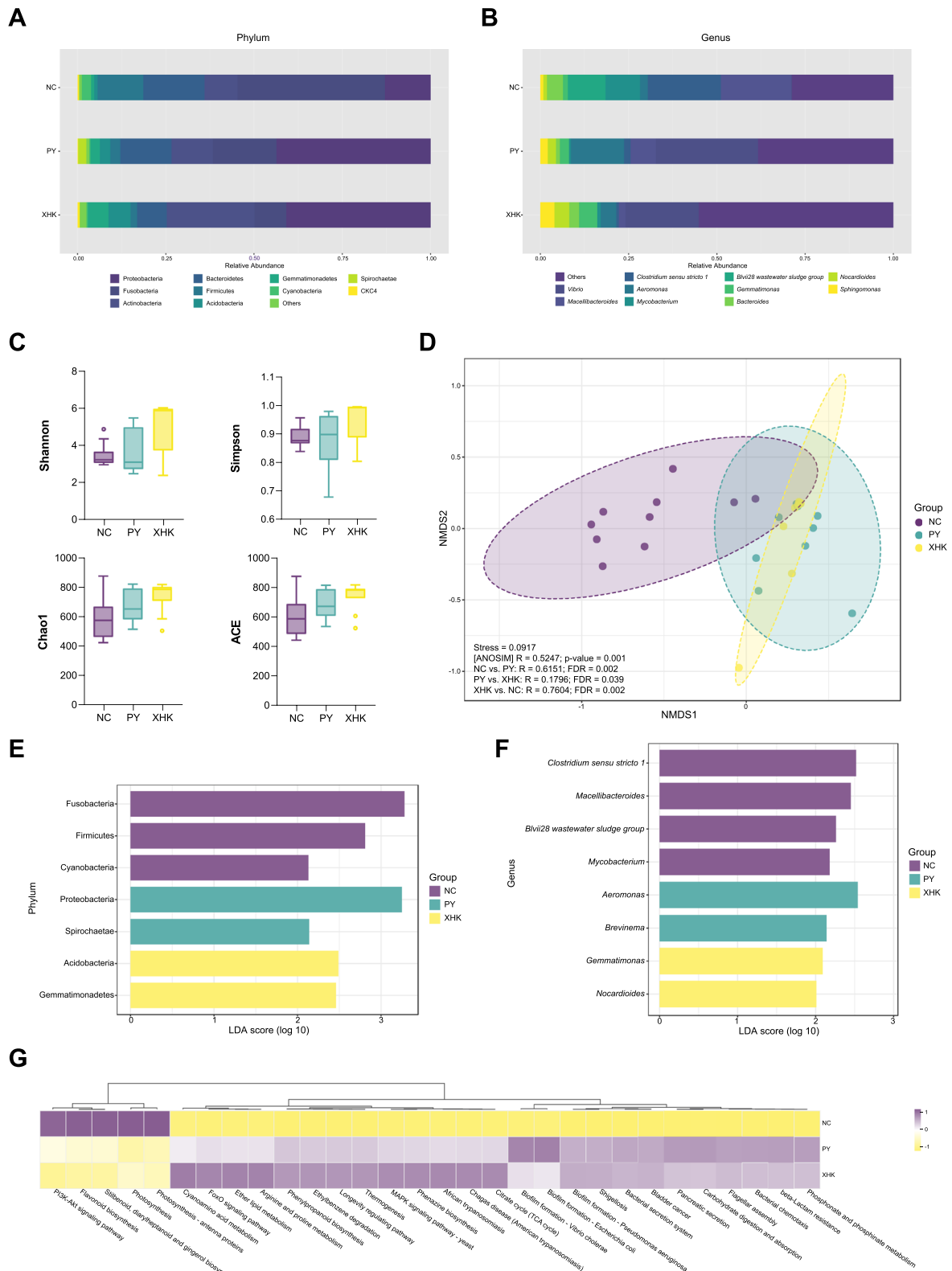


Fig. 2 (See legend on previous page.)

(Kruskal-Wallis test, $FDR < 0.05$) (Additional file 6: Table S2).

At the genus level (Fig. 2B), there were significant differences in the gut microbial communities. For example, the abundance of *Macellibacteroides* was significantly higher in NC than in XHK (Kruskal-Wallis test, $FDR < 0.05$). *Clostridium sensu stricto 1*, *Mycobacterium*, and *Blvii28 wastewater sludge groups* were significantly more abundant in NC (Kruskal-Wallis test, $FDR < 0.05$) than in the other groups, while *Nocardioidea* and *Sphingomonas* were significantly less abundant (Kruskal-Wallis test, $FDR < 0.05$) (Additional file 7: Table S3).

The diversity indices of the gut bacteria, such as Shannon, Simpson, Chao1, and ACE, are shown in Fig. 2C. Overall, the diversity indices in XHK were higher than those in NC and PY. However, there were no significant differences among groups in Shannon (Kruskal-Wallis test, $p = 0.063$), Simpson (Kruskal-Wallis test, $p = 0.070$), Chao1 (Kruskal-Wallis test, $p = 0.093$) and ACE (Kruskal-Wallis test, $p = 0.155$), which indicated that the impact of culture systems on bacterial diversity was limited.

We performed NMDS analysis based on the Bray-Curtis distance to analyze differences in bacterial communities among groups, as shown in Fig. 2D. NC was well separated from the other groups, and PY had a microbial community similar to that of XHK. The stress value ($0.0917 < 0.1$) indicated a stable NMDS model. ANOSIM and multiple comparisons results indicated that every two groups separated significantly (NC vs. PY, $FDR = 0.002$; PY vs. XHK, $FDR = 0.039$; XHK vs. NC, $FDR = 0.002$), and the culture systems had a significant impact on the bacterial community (ANOSIM: $R = 0.5247$; $p = 0.001$).

To determine the indicator taxa among groups, we applied LEfSe and presented the results at the phylum and genus levels in Fig. 2E, F, respectively. The results indicated 7 phyla and 8 genera with a significant difference among the groups ($\log LDA \text{ score} > 2.0$, Kruskal-Wallis test, $FDR < 0.05$). At the phylum level, Fusobacteria, Firmicutes, and Cyanobacteria were significant in NC; Proteobacteria and Spirochaetae were significant in PY; and Acidobacteria and Gemmatimonadetes were significant in XHK (Additional file 1: Fig S1). At the genus level, the indicators were *Clostridium sensu stricto 1*, *Macellibacteroides*, *Blvii28 wastewater sludge group* and *Mycobacterium* in NC; *Aeromonas* and *Brevinema* in PY; and *Gemmatimonas* and *Nocardioidea* in XHK (Additional file 2: Fig S2).

PICRUSt2 was utilized to predict bacterial function in the three groups. A total of 370 pathways were predicted, with 278 pathways identified as significant (Kruskal-Wallis test, $FDR < 0.05$), indicating that culture systems

affected the potential metabolic capacity of gut microbiota. Among the significant pathways, almost half of the pathways were categorized under "metabolism" (131/278, 47.12%). Only a few pathways were classified under "organismal systems" (49/278, 17.63%), "human diseases" (43/278, 15.47%), "cellular processes" (24/278, 8.63%), "environmental information processing" (22/278, 7.91%), and "genetic information processing" (9/278, 3.24%). The top 20 pathways, ranked by p -value, are shown in Fig. 2G, with the most altered pathways being "cyanoamino acid metabolism", "photosynthesis", and "phenylpropanoid biosynthesis".

Metabolic profiling of the gut in bighead carp

A total of 1453 metabolites were detected, with 1168 identified by LC-MS and 285 by GC-MS. These metabolites included 681 lipids and lipid-like molecules, 184 organic acids and derivatives, 95 organic oxygen compounds, 76 organ heterocyclic compounds, 61 benzenoids, 33 phenylpropanoids and polyketides, etc. (Additional file 8: Table S4).

The data were subjected to PCA to compare the three groups' metabolic composition. The PCA score plot (Fig. 3A) could distinguish the three groups. Three principal components (PC1, PC2, and PC3) were extracted, explaining 41%, 14%, and 11% of the variability, respectively.

OPLS-DA was used to analyse the degree of variability in intergroup samples. High predictability (Q^2) and strong goodness of fit (R^2X , R^2Y) were reflected between every two groups (Additional file 9: Table S5), which demonstrated that the models were stable and could be used to identify significantly differential metabolites further. In the OPLS-DA score plots (Fig. 3B–D), every two groups were clearly separated, indicating distinct differences in metabolic profiling between groups. Permutation tests indicated that the models were not overfitted (Additional file 9: Table S5).

Significantly differential metabolites were screened, revealing 710 metabolites in NC compared with PY, 372 metabolites in PY compared with XHK, and 766 metabolites in XHK compared with NC. A total of 93 common significantly differential metabolites were screened in all intergroup comparisons, which included 32 lipids and lipid-like molecules, 19 organic acids and derivatives, and 7 organic oxygen compounds (Fig. 3E).

MetPA was conducted on all these metabolites, which enriched 27 pathways, of which 11 were significant (hypergeometric test, $p < 0.05$) (Additional file 10: Table S6). These pathways included 4 related to amino acid metabolism, 3 to carbohydrate metabolism, 1 pathway to translation, 1 to nucleotide metabolism, 1 to lipid metabolism, and 1 to metabolism of cofactors and

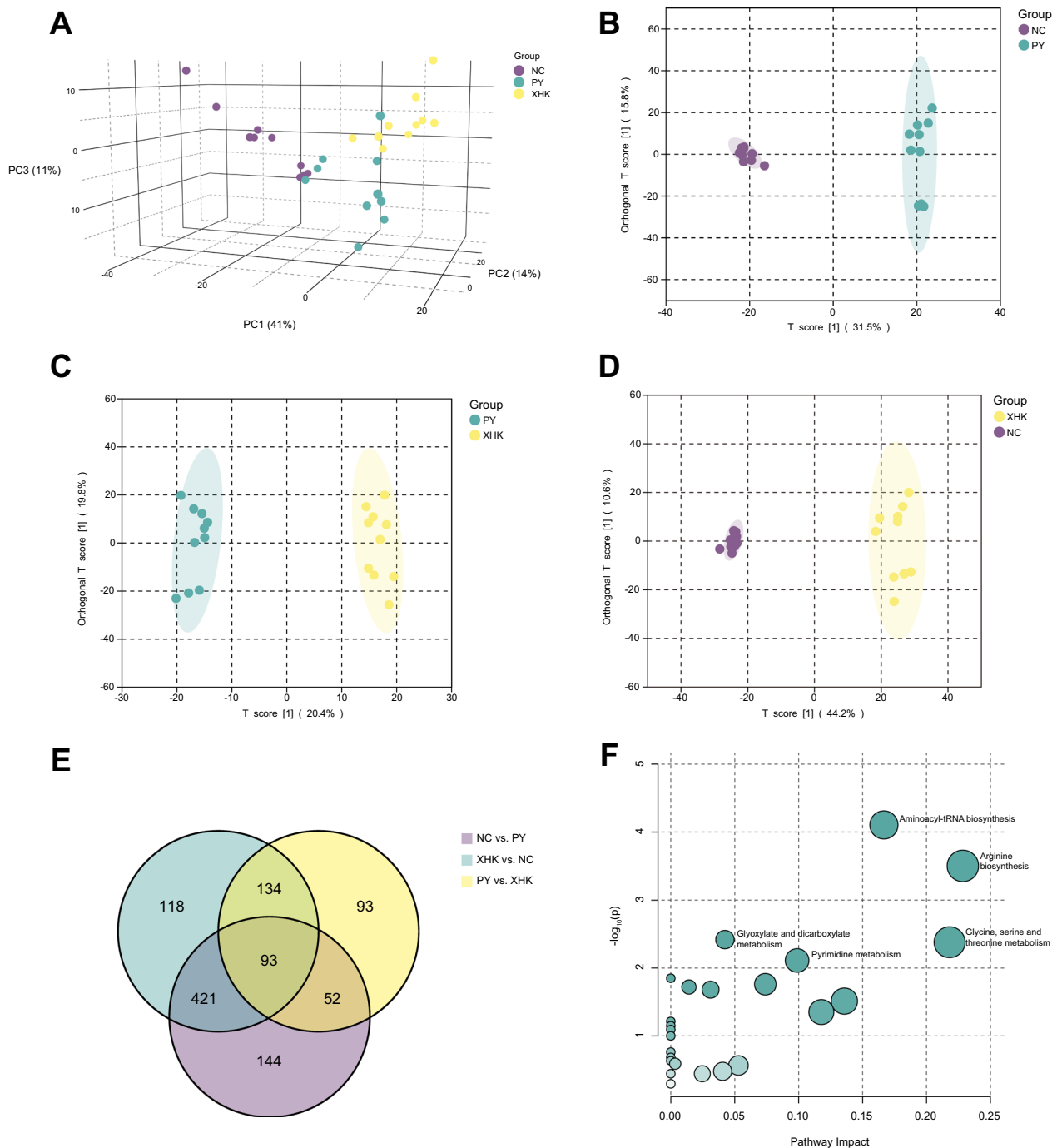


Fig. 3 Multivariate statistical analysis and metabolic pathway analysis of intestinal contents. **A** The PCA score plot clearly separates NC, PY, and XHK, indicating different metabolic profiles among the three groups. **B–D** The OPLS-DA score plots show a clear separation of every two groups, indicating strong effects of the culture systems on the metabolic composition. **E** The Venn diagram shows the number of significantly differential metabolites between groups, with the numbers in circles indicating the number of metabolites and the numbers in overlapping parts representing the number of common metabolites in intergroup comparison. **F** The enriched pathways are shown on a scatter plot, with the horizontal axis indicating the impact of the pathways and the vertical axis indicating the significance of the pathways. The significance and impact of each pathway are represented by the size and colour of the scatter, respectively

vitamins. The significantly altered pathways included "aminoacyl-tRNA biosynthesis", "arginine biosynthesis", "glyoxylate and dicarboxylate metabolism", "glycine, serine, and threonine metabolism", "pyrimidine metabolism" (Fig. 3F).

The relationship between gut microbiota and metabolites

To explore potential associations between significant gut microbes and metabolites under environmental influence, we utilised Spearman rank correlation. At the phylum level, 26 associations between 17 metabolites and 5 microbes were found (Spearman rank correlation, $r > 0.8$, $p < 0.05$) (Fig. 4A). At the genus level, 30 associations were obtained for 6 microbes and 20 metabolites (Spearman rank correlation, $r > 0.8$, $p < 0.05$) (Fig. 4B). The details of the correlation can be seen in Additional file 11: Tables S7 and Additional file 12: Table S8.

The correlation between environmental factors and gut microbiota

Table 1 shows the environmental factors, including water temperature (WT), dissolved oxygen (DO), nitrate nitrogen ($\text{NO}_3\text{-N}$), ammonium nitrogen ($\text{NH}_4\text{-N}$), pH, and transparency, for the three groups in four seasons. PY had the highest water temperature on average, significantly higher than the other two groups. NC had the highest levels of DO, $\text{NO}_3\text{-N}$, $\text{NH}_4\text{-N}$, pH, and transparency, with $\text{NH}_4\text{-N}$ content significantly higher than that in XHK, while other factors were significantly higher than the other groups (Kruskal-Wallis test, $\text{FDR} < 0.05$).

Table 2 presents the contribution of environmental factors to the variation in gut microbiota obtained by VPA. All the variation partitioning fractions were significant in the permutation test ($p < 0.05$). Among the environmental factors, pH explained the most variation in gut microbiota (43.41%), followed by $\text{NH}_4\text{-N}$ (43.14%), DO (38.34%), transparency (34.41%), $\text{NO}_3\text{-N}$ (28.28%), and WT (19.40%).

To further explore the correlation between environmental factors and significant microbes at the phylum and genus levels, redundancy analysis (RDA) was conducted, and the results are shown in Fig. 5. All six canonical axes explain 23.31% of the total variability. The first two axes, which contributed 71.20% and 11.45% of the explained variance ($p < 0.01$), respectively, were used for further analysis.

The results showed that Fusobacteria and *Macellibacteroides* were positively correlated with all environmental factors except transparency. Conversely, Spirochaetae, Acidobacteria, Gemmatimonadetes, *Brevinema*, *Gemmatimonas*, and *Nocardioideis* exhibited an opposite trend. Firmicutes, Cyanobacteria, *Clostridium sensu stricto 1*, *Blvii28 wastewater sludge group*, and *Mycobacterium* positively correlated with $\text{NH}_4\text{-N}$, pH, DO, and $\text{NO}_3\text{-N}$, while exhibiting negative correlations with WT and transparency. On the contrary, Proteobacteria and *Aeromonas* showed the opposite trend.

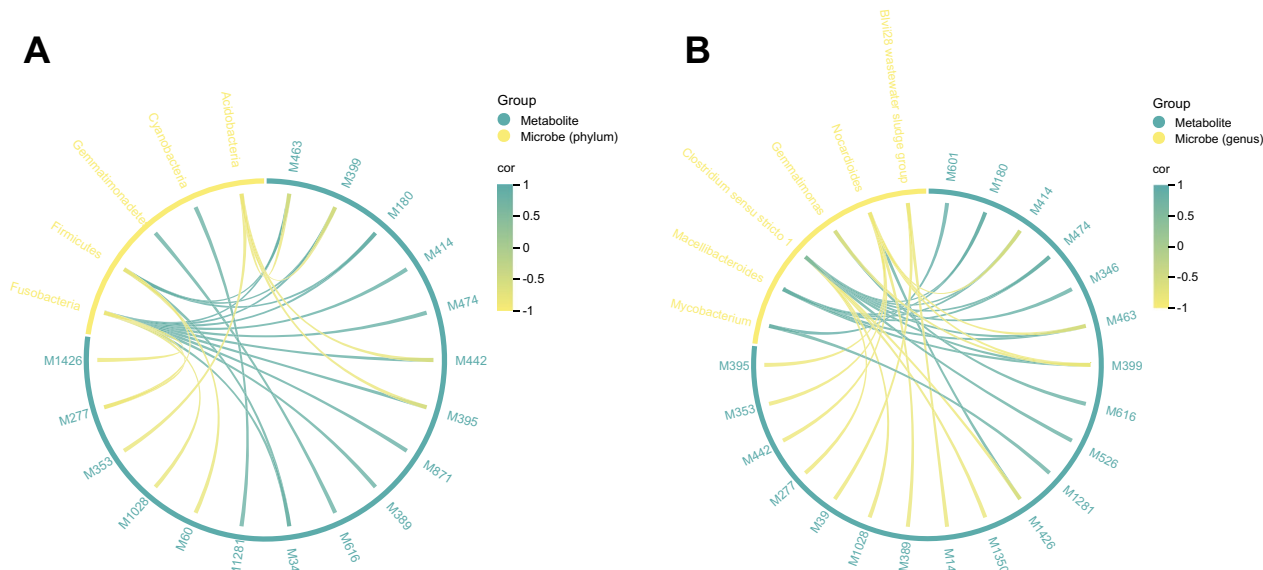


Fig. 4 The correlation of microbes and metabolites. **A** The correlation at the phylum level. **B** The correlation at the genus level. The lines in the circles represent the correlation between metabolites and microbes, with greener colours representing more positive correlations and yellower colours representing more negative correlations

Table 1 Environmental factor parameters for the three groups in four seasons

	Spring (March)			Summer (August)			Autumn (October)			Winter (December)			Average		
	NC	PY	XHK	NC	PY	XHK	NC	PY	XHK	NC	PY	XHK	NC	PY	XHK
WT	14.23 ± 0.05 ^a	12.98 ± 0.40 ^b	13.00 ± 0.17 ^b	30.12 ± 0.65 ^a	30.38 ± 0.41 ^a	28.13 ± 0.38 ^b	22.23 ± 0.23 ^{ab}	23.83 ± 0.82 ^a	21.73 ± 0.26 ^b	6.33 ± 0.96 ^a	15.32 ± 0.34 ^b	10.20 ± 0.27 ^{ab}	18.23 ± 0.21 ^a	20.63 ± 0.20 ^b	18.27 ± 0.07 ^a
DO	11.12 ± 0.85 ^a	8.83 ± 0.12 ^b	8.86 ± 0.30 ^b	9.64 ± 0.17 ^a	7.83 ± 0.64 ^b	8.66 ± 0.35 ^b	11.88 ± 0.17 ^a	8.19 ± 0.21 ^{ab}	7.67 ± 0.26 ^b	8.72 ± 0.50 ^a	7.95 ± 0.95 ^b	7.62 ± 0.23 ^b	10.34 ± 0.25 ^a	8.20 ± 0.28 ^b	8.20 ± 0.07 ^b
NO ₃ -N	0.81 ± 0.03 ^a	0.52 ± 0.07 ^b	0.70 ± 0.11 ^{ab}	0.51 ± 0.04 ^b	0.22 ± 0.02 ^b	0.18 ± 0.04 ^b	0.63 ± 0.03 ^a	0.30 ± 0.05 ^b	0.37 ± 0.10 ^b	0.53 ± 0.05 ^a	0.35 ± 0.06 ^b	0.39 ± 0.05 ^b	0.62 ± 0.03 ^a	0.35 ± 0.03 ^b	0.41 ± 0.05 ^b
NH ₄ ⁺ -N	0.21 ± 0.02 ^a	0.05 ± 0.02 ^b	0.03 ± 0.01 ^b	0.14 ± 0.05 ^a	0.07 ± 0.02 ^{ab}	0.05 ± 0.01 ^b	0.10 ± 0.02 ^a	0.06 ± 0.01 ^{ab}	0.02 ± 0.00 ^b	0.04 ± 0.02 ^a	0.06 ± 0.01 ^b	0.04 ± 0.02 ^a	0.12 ± 0.02 ^a	0.06 ± 0.01 ^{ab}	0.03 ± 0.01 ^b
pH	7.95 ± 0.23 ^a	7.13 ± 0.17 ^b	7.19 ± 0.18 ^b	8.68 ± 0.12 ^a	7.46 ± 0.13 ^b	7.37 ± 0.21 ^b	8.79 ± 0.07 ^a	8.25 ± 0.43 ^a	7.65 ± 0.07 ^b	7.70 ± 0.16 ^a	7.08 ± 0.10 ^b	7.14 ± 0.10 ^b	8.29 ± 0.10 ^a	7.48 ± 0.13 ^b	7.34 ± 0.08 ^b
Trans- par- ency	1.15 ± 0.10 ^a	1.62 ± 0.04 ^b	2.68 ± 0.79 ^b	0.82 ± 0.04 ^a	3.00 ± 0.09 ^b	1.15 ± 0.08 ^c	1.37 ± 0.05 ^a	2.30 ± 0.18 ^b	2.68 ± 0.37 ^b	1.57 ± 0.05 ^a	2.13 ± 0.19 ^b	2.12 ± 0.08 ^b	1.22 ± 0.03 ^a	2.26 ± 0.04 ^b	2.16 ± 0.16 ^b

There is a significant difference between the groups denoted by different letters

Table 2 The relative contributions of environmental factors to variation in gut microbiota

Environmental factors	Variance explained	Sig
pH	0.4341	0.001***
NH ₄ -N	0.4314	0.001***
DO	0.3834	0.001***
Transparency	0.3441	0.003**
NO ₃ -N	0.2828	0.001***
WT	0.19398	0.022*

Significance levels with *, **, and *** represent p-value < 0.05, 0.01, and 0.001 between groups, respectively (permutation test)

Discussion

This study demonstrates the impact of culture systems on the gut microbiota and metabolic profiles of bighead carp.

Culture systems greatly influence the gut microbiota of bighead carp.

In the current study, the dominant phyla in bighead carp's gut microbiota were Proteobacteria, Fusobacteria, Actinobacteria, Bacteroidetes, and Firmicutes, consistent with previous findings in marine and freshwater fishes [11, 57–59] and supporting Luo's research on bighead carp [21]. Among all phyla, especially Cyanobacteria, it is considered to be directly consumed by filter-feeding fish [60]. As a filter-feeding planktivorous carp, bighead carp easily filter some colony-forming cyanobacteria [27, 61, 62]. The abundance of Cyanobacteria in the hindgut was significantly higher in NC than in the other two groups (Additional file 1: Fig S1C), possibly due to differences in food sources in the three culture systems.

Alpha and beta diversity are important parameters used to evaluate the structural characteristics of microbiota. In our study, gut microbiota diversity and richness were higher in alpine cold-water reservoirs and inner lakes than in ponds, consistent with other research [9, 11, 63, 64]. This could be due to larger habitats providing a wider range of diets. Therefore, fish may be constantly exposed to more bacteria [65].

Beta diversity analysis revealed significant differences in the gut microbial communities of bighead carp in all three culture systems, in agreement with other studies [9, 11]. This may be due to culture environments, diet, and genetics [66]. The VPA results showed that environmental factors explained up to 43.41% of the variation in the gut microbiota, which indicates a great influence of environmental factors. Diet is considered a critical factor in regulating the gut microbiota composition [67], and different bait provided by different culture systems could be

an important reason for the differences in gut microbiota diversity. The bighead carp used in our study were from the same batch reared in the same hatchery and shared a similar genetic background, so the effect from the genetic background was relatively small. Therefore, we believe that differences in environmental factors and diet were the main causes of the significant differences observed.

LefSe analysis revealed 15 biomarkers that may cause significant differences in communities. At the phylum level, these included Fusobacteria, Firmicutes, Cyanobacteria, Proteobacteria, Spirochaetae, Acidobacteria, and Gemmatimonadetes; at the genus level, these included *Clostridium sensu stricto 1*, *Macellibacteroides*, *Blvii28 wastewater sludge group*, *Mycobacterium*, *Aeromonas*, *Brevinema*, *Gemmatimonas*, and *Nocardioidea*. *Clostridium* is typically considered the most efficient lignocellulose degrader due to the presence of multienzyme complexes [68, 69] consisting of multiple cellulases and hemicellulases in combination with enzyme-free scaffoldin [70–72] that synergistically and efficiently degrade lignocellulose. They also contribute to the host's nutrition by supplying fatty acids and vitamins [73]. *Macellibacteroides* are capable of decomposing cellulose- and hemicellulose-derived sugars [74]. Several species of *Aeromonas* can produce cellulase [75] and have intensive cellulolytic activity [76, 77]. Although bighead carp are important plankton feeders [78], they lack the cellulase enzyme that breaks down the cell walls of algae in their gut [79]. We hypothesise that the cellulolytic action of these bacteria compensates for this deficiency in bighead carp and that bighead carp derive energy and nutrients from this process [27]. The abundance of both *Clostridium sensu stricto 1* and *Macellibacteroides* was positively correlated with the long and short diameter of muscle fibres (Spearman Rank Correlation). These may suggest that the culture systems improve nutrition levels and muscle quality in bighead carp by affecting gut microbes.

PICRUSt2 is a tool used for metagenome prediction to predict the approximate functional potential of a community [48]. In our study, 278 significantly different KEGG pathways were predicted, most of which were involved in metabolism, and organic systems, revealing the possible functional mechanisms of culture systems affecting gut microbes.

In conclusion, the culture systems significantly alter the community structure of gut microbiota and potentially impact their metabolic profiling.

Culture systems have a significant impact on gut metabolic profiling.

Gut metabolites are the outcome of the joint metabolism of the host and microbial community and can reflect the

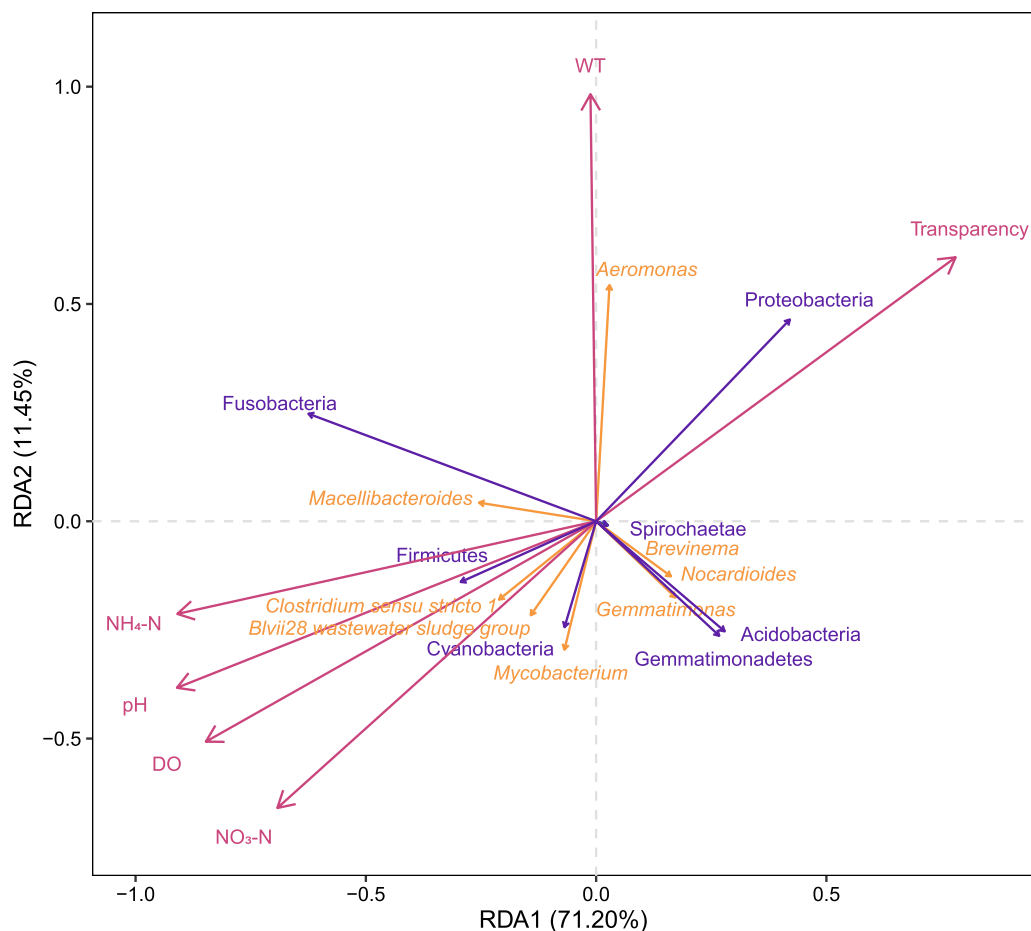


Fig. 5 The correlation among samples, environmental factors, and significant microbes. Blue and yellow arrows indicate vectors of significant microbes at the phylum and genus levels, respectively, while red arrows represent vectors of environmental factors. A positive correlation is indicated when the angle between vectors is less than 90° , while a negative correlation is indicated when it is greater than 90° . The vectors are perpendicular to each other to indicate irrelevance

outcomes of nutrient uptake, digestion, and absorption by the gut microbiota [80].

In this study, multivariate statistical analyses, including PCA and OPLS-DA, revealed significant changes in the intestinal metabolite profile of bighead carp under different culture environments, reflecting the significant influence of the environment on the joint metabolism of host and gut microbes.

Further exploration of the differential metabolites showed that 93 key metabolites were significantly enriched in 11 pathways, of which 4 were related to amino acid metabolism and 1 to translation, including "aminoacyl-tRNA biosynthesis", "arginine biosynthesis", "glycine, serine, and threonine metabolism", "alanine, aspartate, and glutamate metabolism", and "cysteine and methionine metabolism". The enriched pathways suggest that the culture systems exerted an important impact on host-microbe joint metabolism in the gut, particularly on

amino acid metabolism and protein translation-related metabolic pathways.

Overall, the culture systems significantly altered intestinal metabolism.

Potential association of fish muscle quality with microbes and metabolites in the gut

Several studies have demonstrated the beneficial role of gut microbes in improving muscle quality. For example, mice supplemented with *Lactobacillus plantarum* were accompanied by a change in muscle fibre type, that is, a significant increase in the proportion of type I fibres in the gastrocnemius muscle [13]. And when gut microbiota from obese Rongchang pigs and lean Yorkshire pigs were transferred to germ-free mice by faecal transplantation, mice fed Rongchang pig faeces tended to have increased body fat weight, increased percentage of slow muscle

fibres, decreased diameter and cross-sectional area of the gastrocnemius muscle, and increased fat in gastrocnemius muscle compared to the mice fed Yorkshire pig faeces [14]. However, the mechanisms underlying these effects are not well understood.

Amino acids are important components of fish muscle quality [81]. Intestinal microorganisms regulate amino acids mainly through two mechanisms. On the one hand, microbes can utilise amino acids, producing acetic acid [82], propionic acid, butyric acid [83], hydrogen sulfide (H₂S) [83, 84], polyamine [85], phenolic and indole compounds [86]. These metabolites play a crucial role in regulating host physiology [87]. However, this process exists in the large intestine and is largely not absorbed by the colonic mucosa [88], making it difficult to influence the host's amino acid metabolism. On the other hand, intestinal microbes can synthesise amino acids de novo [89]. Numerous reports of microbes synthesising amino acids affect the host's amino acid metabolism; for example, microbial lysine can be incorporated into host proteins, as observed in uremic patients and subjects consuming a low-protein diet [90, 91]. The significant contribution of microbial-derived lysine and threonine to free plasma lysine and threonine has also been observed in studies of nitrogen (protein)-sufficient diets in adults [89, 92]. In pigs fed diets incorporating 15N-NH₄Cl and 14C-polyglucose, microbially produced amino acids such as valine, isoleucine, leucine, phenylalanine, and lysine were found to be incorporated into human proteins [93] and absorbed mainly from the small intestine [93, 94]. In the present study, we found that L-cysteine, L-lysine, and L-threonine differed significantly among the three groups (Kruskal-Wallis test, FDR < 0.05) (Additional file 3: Fig S3A, S3B, S3C), and their levels were positively correlated with muscle quality. We suggest that these amino acids may be synthesised de novo by gut microbes and absorbed by the host, affecting the changes in amino acids in fish muscle and thus improving the quality of fish muscle.

Based on this hypothesis, we established the association between gut microbes and relevant metabolites using Spearman Rank Correlation with a cutoff of $r > 0.65$ and consequently inferred which microbes perform the corresponding functions using the R corr package. According to the analysis, several bacteria, including *uncultured Chloroflexi bacterium*, *Pedobacter*, *Azohydromonas*, *Sinomonas*, *Patulibacter*, *Sorangium*, *Altererythrobacter*, and *Bryobacter*, may be potential amino acid-synthesising bacteria, as shown in Additional file 4: Fig S4. However, it's important to note that these findings are based on inference and correlation, and further experimental validation would be necessary to confirm these associations.

Additionally, certain metabolites may contribute to improving muscle quality in fish, such as glutamine which can increase the activity of the mammalian target of rapamycin (mTOR), a protein kinase that regulates protein synthesis in animal tissues and cells [95]. Although not yet available for fish [96], our study found that glutamine was the most abundant metabolite in the XHK group, followed by PY and NC (Additional file 3: Fig S3D), which is consistent with the muscle quality revealed by muscle microstructure. This suggests that glutamine could be a potential metabolite to enhance muscle quality in fish.

The flavour is one of the most important factors in influencing the edible quality of fish [97]. Nucleotides are a taste-active substance [98], among which the nucleotides inosine-5'-monophosphate (5'-IMP) and adenosine-5'-monophosphate (5'-AMP) contribute significantly to umami taste. They work in synergy with glutamate to intensify the taste sensation by binding to the same receptors, taste receptor type 1 members 1 and 3 [99, 100]. In our previous study, bighead carp in XHK exhibited a stronger umami intensity compared to other groups [12]. IMP is also considered an umami substance for fish products [101]. In the current study, 5'-IMP and glutamate followed the same trend of differences among the groups (Kruskal-Wallis test, FDR < 0.05) (Additional file 3: Fig S3E, S3F). This indicates that 5'-IMP and glutamate are probably the metabolites responsible for making the muscle of bighead carp tastier.

These findings suggest that gut microbiota and metabolites may play important roles in determining muscle quality in fish. This provides a practical direction for future research to improve the muscle quality of bighead carp. To verify the role of these gut microbes and metabolites, we may isolate and extract intestinal flora and conduct transplantation in aseptic mice, as well as supplement metabolites.

Conclusions

It is evident that culture systems significantly impact the intestinal microbiota and metabolites of bighead carp. Our findings demonstrate that the culture systems not only alter the gut microbial community of bighead carp, with notable variations in community structure, abundance, and potential metabolic functions, but also affect host gut metabolism, particularly with significant enrichment in pathways related to amino acid metabolism. Moreover, we discuss potential mechanisms that may impact muscle quality. We hypothesize that significantly different amino acids in the gut are the primary cause of the effect on muscle quality. Based on this hypothesis, we suggest that gut microbes may play a role in altering

muscle quality in fish through the biosynthesis of amino acids.

Further investigation into the potential association between fish muscle quality and gut microbes and metabolites can provide a foundation for enhancing big-head carp's muscle quality and nutritional value.

Abbreviations

NC	Nancheng
PY	Poyang
XHK	Xiahuikeng
DNA	Deoxyribonucleic acid
WT	Water temperature
DO	Dissolved oxygen
NO ₃ -N	Nitrate nitrogen
NH ₄ -N	Ammonium nitrogen
16S rRNA	16S ribosomal ribonucleic acid rRNA
PCR	Polymerase chain reaction
QIIME	Quantitative insights into microbial ecology
OTU	Operational taxonomic units
NMDS	Non-metric multidimensional scaling
ANOSIM	A one-way analysis of similarity
LEFSe	Linear discriminant analysis Effect Size
LDA	Linear discriminant analysis
FDR	False discovery rate
PICRUST2	Phylogenetic investigation of communities by reconstruction of unobserved states
LC-MS	Liquid chromatograph-mass spectrometer
GC-MS	Gas chromatograph-mass spectrometer
QC	Quality control
MS	Mass spectrum
RSD	Relative standard deviation
PCA	Principal component analysis
OPLS-DA	Orthogonal projections to latent structures-discriminant analysis
VIP	Variable importance in projection
MetPA	Metabolic pathway analysis
VPA	Variation partitioning analysis
RDA	Redundancy analysis

Supplementary Information

The online version contains supplementary material available at <https://doi.org/10.1186/s42523-023-00239-7>.

Additional file 1. Fig S1. The relative abundance of indicator taxa at the phylum level. (A) Fusobacteria. (B) Firmicutes. (C) Cyanobacteria. (D) Proteobacteria. (E) Spirochaetae. (F) Acidobacteria. (G) Gemmatimonadetes. Significance levels with *, **, and *** represent FDR < 0.05, 0.01, and 0.001 between groups, respectively (Kruskal-Wallis test).

Additional file 2. Fig S2. The relative abundance of indicator taxa at the genus level. (A) *Clostridium sensu stricto 1*. (B) *Macellibacteroides*. (C) *Blvii28 wastewater sludge group*. (D) *Mycobacterium*. (E) *Aeromonas*. (F) *Brevinema*. (G) *Gemmatimonas*. (H) *Nocardioideis*. Significance levels with *, **, and *** represent FDR < 0.05, 0.01, and 0.001 between groups, respectively (Kruskal-Wallis test).

Additional file 3. Fig S3. Normalised peak intensity of potential metabolites which influence fish muscle quality (A) L-cysteine. (B) L-lysine. (C) L-threonine. (D) glutamine. (E) 5'-IMP. (F) L-glutamate. Significance levels with *, **, and *** represent FDR < 0.05, 0.01, and 0.001 between groups, respectively (Kruskal-Wallis test).

Additional file 4. Fig S4. Potential microbes synthesising amino acids. The curves represent the correlation between metabolites and microbes, with greener colours representing stronger positive correlations and yellow-lower colours representing stronger negative correlations.

Additional file 5. Table S1. The abundance and taxonomy of OTUs.

Additional file 6. Table S2. The abundance and significance of top 10 microbes at the phylum level.

Additional file 7. Table S3. The abundance and significance of top 10 microbes at the genus level.

Additional file 8. Table S4. The abundance and classification of metabolites.

Additional file 9. Table S5. The parameters and evaluation of PCA and OPLS-DA models.

Additional file 10. Table S6. The significance and impact of enriched pathways.

Additional file 11. Table S7. The potential metabolites and microbes at the phylum level.

Additional file 12. Table S8. The potential metabolites and microbes at the genus level.

Acknowledgements

We appreciate the assistance of Liuzheng Wu, Jin Li, Rui Xiao, Yaying Huang, Feng Jin, Bin Sheng, and Runming Guo for the experiments and manuscript.

Author contributions

BH and YH conceived and designed the experiments. CY, HG and BH conducted the experiments. CY analysed the experimental data and wrote the manuscript. SG, YZ, HQ, and JZ made the paraffin sections. QZ, YZ, DW, and GY provided the study ideas. All authors read and approved the final manuscript.

Funding

This work was supported by China Agriculture Research System No. 49 (CARS-49) and the Key Research Development Program of the Jiangxi Province of China (20212BBF61010).

Availability of data and materials

The 16S sequencing data were deposited into the National Center of Biotechnology Information (NCBI) Sequence Read Archive (SRA) database under Accession PRJNA933520. Data generated or analysed during this study are included in this published article and its supplementary information files.

Declarations

Ethics approval and consent to participate

The authors declare that all experiments involving bighead carp were ethical. All our experiments were conducted in compliance with the standard ethical guidelines and under the control of Nanchang University.

Consent for publication

Not applicable.

Competing interests

The authors declare that they have no competing interests.

Author details

¹School of Life Science, Nanchang University, Nanchang 330031, China. ²Jiangxi Province Key Laboratory of Aquatic Animal Resources and Utilization, Nanchang University, Nanchang 330031, China. ³Jiangxi Provincial Aquatic Biology Protection and Rescue Center, Nanchang 330000, China. ⁴Modern Agricultural Research Institute, Nanchang University, Nanchang 330031, China.

Received: 21 October 2022 Accepted: 8 March 2023

Published online: 01 April 2023

References

- Xiong JB, Nie L, Chen J. Current understanding on the roles of gut microbiota in fish disease and immunity. *Zool Res.* 2019;40:70–6.

2. Rawls JF, Mahowald MA, Goodman AL, Trent CM, Gordon JJ. In vivo imaging and genetic analysis link bacterial motility and symbiosis in the zebrafish gut. *Proc Natl Acad Sci U S A*. 2007;104:7622–7.
3. Koch BEV, Yang S, Lamers G, Stougaard J, Spaink HP. Intestinal microbiome adjusts the innate immune setpoint during colonization through negative regulation of MyD88. *Nat Commun*. 2018;9:4099.
4. Smith TB, Wahl DH, Mackie RI. Volatile fatty acids and anaerobic fermentation in temperate piscivorous and omnivorous freshwater fish. *J Fish Biol*. 1996;48:829–41.
5. Ni J, Yan Q, Yu Y, Zhang T. Factors influencing the grass carp gut microbiome and its effect on metabolism. *FEMS Microbiol Ecol*. 2014;87:704–14.
6. Semova I, Carten JD, Stombaugh J, Mackey LC, Knight R, Farber SA, Rawls JF. Microbiota regulate intestinal absorption and metabolism of fatty acids in the zebrafish. *Cell Host Microbe*. 2012;12:277–88.
7. Bereded NK, Abebe GB, Fanta SW, Curto M, Waidbacher H, Meimberg H, Domig KJ. The gut bacterial microbiome of Nile tilapia (*Oreochromis niloticus*) from lakes across an altitudinal gradient. *BMC Microbiol*. 2022;22:87.
8. Bereded NK, Abebe GB, Fanta SW, Curto M, Waidbacher H, Meimberg H, Domig KJ. The impact of sampling season and catching site (wild and aquaculture) on gut microbiota composition and diversity of Nile tilapia (*Oreochromis niloticus*). *Biology (Basel)*. 2021;10:180.
9. Sun P, Zhang H, Jiang Y, Gao Q, Tang B, Ling J, Yuan X. Relationships between the gut microbiota of juvenile black sea bream (*Acanthopagrus schlegelii*) and Associated environment compartments in different habitats. *Microorganisms*. 2021;9:2557.
10. Duan J, Xu D, Liu K, Zhou Y, Xu P. Diversity of intestinal microbiota in *Coilia ectenes* from Lake Taihu, China. *Open Life Sci*. 2017;12:315–25.
11. Dulski T, Kozłowski K, Ciesielski S. Habitat and seasonality shape the structure of tench (*Tinca tinca* L.) gut microbiome. *Sci Rep*. 2020;10:4460.
12. Hu B, Zhou J, Qiu H, Lai X, Li J, Wu D, Sheng J, Hong Y. Comparison of nutritional quality and volatile flavor compounds among bighead carp from three aquaculture systems. *Saudi J Biol Sci*. 2021;28:4291–9.
13. Chen YM, Wei L, Chiu YS, Hsu YJ, Tsai TY, Wang MF, Huang CC. *Lactobacillus plantarum* TWK10 supplementation improves exercise performance and increases muscle mass in mice. *Nutrients*. 2016;8:205.
14. Yan H, Diao H, Xiao Y, Li W, Yu B, He J, Yu J, Zheng P, Mao X, Luo Y, et al. Gut microbiota can transfer fiber characteristics and lipid metabolic profiles of skeletal muscle from pigs to germ-free mice. *Sci Rep*. 2016;6:31786.
15. Wang Y, Yao J, Luo Y, Tan H, Huang X, Wang S, Qin Q, Zhang C, Tao M, Dabrowski K, Liu S. Two new types of homodiploid fish and polyploid hybrids derived from the distant hybridization of female koi carp and male bighead carp. *Mar Biotechnol*. 2021;23:628–40.
16. Li X, Yu Y, Li C, Yan Q. Comparative study on the gut microbiotas of four economically important Asian carp species. *Sci China Life Sci*. 2018;61:696–705.
17. Chen J, Xie P, Zhang D, Lei H. In situ studies on the distribution patterns and dynamics of microcystins in a biomanipulation fish—bighead carp (*Aristichthys nobilis*). *Environ Pollut*. 2007;147:150–7.
18. Li D, Zhao H, Muhammad AI, Song L, Guo M, Liu D. The comparison of ultrasound-assisted thawing, air thawing and water immersion thawing on the quality of slow/fast freezing bighead carp (*Aristichthys nobilis*) filets. *Food Chem*. 2020;320: 126614.
19. Tong J, Sun X. Genetic and genomic analyses for economically important traits and their applications in molecular breeding of cultured fish. *Sci China Life Sci*. 2015;58:178–86.
20. FAO: The State of World Fisheries and Aquaculture 2022. Towards Blue Transformation. 2022.
21. Luo M, An R, Fu J, Wan S, Zhu W, Wang L, Dong Z. Comparative analysis of the gut microbiota in bighead carp under different culture patterns. *J Appl Microbiol*. 2022;132:1357–69.
22. Li T, Long M, Gatesoupe F-J, Zhang Q, Li A, Gong X. Comparative analysis of the intestinal bacterial communities in different species of carp by pyrosequencing. *Microb Ecol*. 2015;69:25–36.
23. Zhu L, Zhang Z, Chen H, Lamer JT, Wang J, Wei W, Fu L, Tang M, Wang C, Lu G. Gut microbiomes of bigheaded carps and hybrids provide insights into invasion: a hologenome perspective. *Evol Appl*. 2021;14:735–45.
24. Meng L-J, Zhang Y, Li X-X, Liu J-H, Wen B, Gao J-Z, Chen Z-Z. Comparative analysis of bacterial communities of water and intestines of silver carp (*Hypophthalmichthys molitrix*) and bighead carp (*H. nobilis*) reared in aquaculture pond systems. *Aquaculture*. 2021;534:736334.
25. Li XM, Zhu YJ, Yan QY, Ringø E, Yang DG. Do the intestinal microbiotas differ between paddlefish (*Polyodon spathala*) and bighead carp (*Aristichthys nobilis*) reared in the same pond? *J Appl Microbiol*. 2014;117:1245–52.
26. Yuan J, Wang Z, Wang B, Mei H, Zhai X, Zhuang Z, Chen M, Zhang Y. Non-specific immunity associated gut microbiome in *Aristichthys nobilis* under different rearing strategies. *Genes (Basel)*. 2021;12:916.
27. Borsodi AK, Szabó A, Krett G, Felföldi T, Specziár A, Boros G. Gut content microbiota of introduced bigheaded carps (*Hypophthalmichthys* spp.) inhabiting the largest shallow lake in Central Europe. *Microbiol Res*. 2017;195:40–50.
28. Lu Y, Zhang P, Li W, Liu J, Shang X, Cheng Y, Li Y. Comparison of gut microbial communities, free amino acids or fatty acids contents in the muscle of wild *Aristichthys nobilis* from Xinlicheng reservoir and Chagan lake. *BMC Microbiol*. 2022;22:32.
29. Yuan L, Wang L, Li Z-H, Zhang M-Q, Shao W, Sheng G-P. Antibiotic resistance and microbiota in the gut of Chinese four major freshwater carp from retail markets. *Environ Pollut*. 2019;255: 113327.
30. Su C, Hu W, Hu Z, Zhang Z, Wedchaparn O, Liangjie Z, Liu Q. Comparison of high-throughput sequencing analysis of gut contents between silver carp *Hypophthalmichthys molitrix* and bighead carp *Hypophthalmichthys nobilis* in mesotrophic and eutrophic lakes. *Mar Freshw Res*. 2019;71:761–70.
31. Guo Y, Bai J, Chang O, Lao H, Ye X, Luo J. Molecular structure of the largemouth bass (*Micropterus salmoides*) Myf5 gene and its effect on skeletal muscle growth. *Mol Biol Rep*. 2009;36:1497–504.
32. Stringer C, Wang T, Michaelos M, Pachitariu M. Cellpose: a generalist algorithm for cellular segmentation. *Nat Methods*. 2021;18:100–6.
33. Schindelin J, Arganda-Carreras I, Frise E, Kaynig V, Longair M, Pietzsch T, Preibisch S, Rueden C, Saalfeld S, Schmid B, et al. Fiji: an open-source platform for biological-image analysis. *Nat Methods*. 2012;9:676–82.
34. Kumar PS, Brooker MR, Dowd SE, Camerlengo T. Target region selection is a critical determinant of community fingerprints generated by 16S pyrosequencing. *PLoS ONE*. 2011;6: e20956.
35. Bolger AM, Lohse M, Usadel B. Trimmomatic: a flexible trimmer for Illumina sequence data. *Bioinformatics*. 2014;30:2114–20.
36. Magoč T, Salzberg SL. FLASH: fast length adjustment of short reads to improve genome assemblies. *Bioinformatics (Oxford, England)*. 2011;27:2957–63.
37. Caporaso JG, Kuczynski J, Stombaugh J, Bittinger K, Bushman FD, Costello EK, Fierer N, Peña AG, Goodrich JK, Gordon JJ, et al. QIIME allows analysis of high-throughput community sequencing data. *Nat Methods*. 2010;7:335–6.
38. Rognes T, Flouri T, Nichols B, Quince C, Mahé F. VSEARCH: a versatile open source tool for metagenomics. *PeerJ*. 2016;4: e2584.
39. Quast C, Pruesse E, Yilmaz P, Gerken J, Schweer T, Yarza P, Peplies J, Glöckner F. The SILVA ribosomal RNA gene database project: improved data processing and web-based tools. *Nucleic Acids Res*. 2013;41:D590–6.
40. Wang Q, Garrity GM, Tiedje JM, Cole JR. Naive Bayesian classifier for rapid assignment of rRNA sequences into the new bacterial taxonomy. *Appl Environ Microbiol*. 2007;73:5261–7.
41. Chong J, Liu P, Zhou G, Xia J. Using MicrobiomeAnalyst for comprehensive statistical, functional, and meta-analysis of microbiome data. *Nat Protoc*. 2020;15:799–821.
42. Kruskal JB. Non-metric multidimensional scaling: a numerical method. *Psychometrika*. 1964;29:115–29.
43. Clarke KR. Non-parametric multivariate analyses of changes in community structure. *Aust J Ecol*. 1993;18:117–43.
44. Warton DI, Wright ST, Wang Y. Distance-based multivariate analyses confound location and dispersion effects. *Methods Ecol Evol*. 2012;3:89–101.

45. Oksanen J, Blanchet FG, Kindt R, Legendre P, Minchin P, O'Hara RB, Simpson G, Solymos P, Stevens MHH, Wagner H. Vegan: community ecology package. R package version 20-3 2011, 2.
46. Goslee S, Urban D. The ECODEST package for dissimilarity-based analysis of ecological data. *J Stat Softw.* 2007;22:1–19.
47. Segata N, Izard J, Waldron L, Gevers D, Miropolsky L, Garrett WS, Huttenhower C. Metagenomic biomarker discovery and explanation. *Genome Biol.* 2011;12:R60.
48. Douglas G, Maffei V, Zaneveld J, Yurgel S, Brown J, Taylor C, Huttenhower C, Langille M. PICRUSt2: an improved and extensible approach for metagenome inference. 2019.
49. Wishart DS, Guo A, Oler E, Wang F, Anjum A, Peters H, Dizon R, Sayeeda Z, Tian S, Lee BL, et al. HMDB 5.0: the Human Metabolome Database for 2022. *Nucleic Acids Res.* 2022;50:D622–31.
50. Fahy E, Subramaniam S, Murphy RC, Nishijima M, Raetz CRH, Shimizu T, Spener F, van Meer G, Wackelam MJO, Dennis EA. Update of the LIPID MAPS comprehensive classification system for lipids1. *J Lipid Res.* 2009;50:S9–14.
51. Smith CA, O'Maille G, Want EJ, Qin C, Trauger SA, Brandon TR, Custodio DE, Abagyan R, Siuzdak G. METLIN: a metabolite mass spectral database. *Ther Drug Monit.* 2005;27:747–51.
52. Pang Z, Chong J, Zhou G, de Lima Morais DA, Chang L, Barrette M, Gauthier C, Jacques P, Li S, Xia J. MetaboAnalyst 5.0: narrowing the gap between raw spectra and functional insights. *Nucleic Acids Res.* 2021;49:388–96.
53. Trygg J, Wold S. Orthogonal projections to latent structures (O-PLS). *J Chemom.* 2002;16:119–28.
54. Pinto RC, Trygg J, Gottfries J. Advantages of orthogonal inspection in chemometrics. *J Chemom.* 2012;26:231–5.
55. Revelle W: psych: procedures for psychological, psychometric, and personality research. R Package Version 1.0–95. Evanston, Illinois 2013.
56. Team RC. R: a language and environment for statistical computing. MSOR connections 2014, 1.
57. Kashinskaya EN, Simonov EP, Kabilov MR, Izvekova GI, Andree KB, Solov'yev MM. Diet and other environmental factors shape the bacterial communities of fish gut in an eutrophic lake. *J Appl Microbiol.* 2018;125:1626–41.
58. Maji UJ, Mohanty S, Mahapatra AS, Mondal HK, Samanta M, Maiti NK. Exploring the gut microbiota composition of Indian major carp, rohu (*Labeo rohita*), under diverse culture conditions. *Genomics.* 2022;114:110354.
59. Yukgehaish K, Kumar P, Sivachandran P, Marimuthu K, Arshad A, Paray BA, Arockiaraj J. Gut microbiota metagenomics in aquaculture: factors influencing gut microbiome and its physiological role in fish. *Rev Aquac.* 2020;12:1903–27.
60. Xie P, Liu J. Practical success of biomanipulation using filter-feeding fish to control cyanobacteria blooms: a synthesis of decades of research and application in a subtropical hypereutrophic lake. *TheScientificWorldJOURNAL.* 2001;1:276487.
61. Zhang Z, Shi Y, Zhang J, Liu Q. Experimental observation on the effects of bighead carp (*Hypophthalmichthys nobilis*) on the plankton and water quality in ponds. *Environ Sci Pollut Res.* 2022;29:56658–75.
62. Xie P. Gut contents of bighead carp (*Aristichthys nobilis*) and the processing and digestion of algal cells in the alimentary canal. *Aquaculture.* 2001;195:149–61.
63. Ruzauskas M, Armalytė J, Lastauskienė E, Šiuoždinienė R, Klimienė I, Mockeliūnas R, Bartkienė E. Microbial and antimicrobial resistance profiles of microbiota in common carps (*Cyprinus carpio*) from aquacultured and wild fish populations. *Animals (Basel).* 2021;11:929.
64. Tan CK, Natrah I, Suyub IB, Edward MJ, Kaman N, Samsudin AA. Comparative study of gut microbiota in wild and captive Malaysian Mahseer (*Tor tambroides*). *Microbiologyopen.* 2019;8: e00734.
65. Dehler CE, Secombes CJ, Martin SAM. Environmental and physiological factors shape the gut microbiota of Atlantic salmon parr (*Salmo salar* L.). *Aquaculture.* 2017;467:149–57.
66. Liu Y, Li Y, Li J, Zhou Q, Li X. Gut microbiome analyses of wild migratory freshwater fish (*Megalobrama terminalis*) through geographic isolation. *Front Microbiol.* 2022;13: 858454.
67. Li Z, Zhang X, Aweya JJ, Wang S, Hu Z, Li S, Wen X. Formulated diet alters gut microbiota compositions in marine fish *Nibea coibor* and *Nibea diacanthus*. *Aquac Res.* 2019;50:126–38.
68. Demain AL, Newcomb M, Wu JH. Cellulase, clostridia, and ethanol. *Microbiol Mol Biol Rev.* 2005;69:124–54.
69. Liu L, Jiao J-Y, Fang B-Z, Lv A-P, Ming Y-Z, Li M-M, Salam N, Li W-J. Isolation of *Clostridium* from Yunnan-Tibet hot springs and description of *Clostridium thermarum* sp. Nov. with lignocellulosic ethanol production. *Syst Appl Microbiol.* 2020;43:126104.
70. Bayer EA, Belaich JP, Shoham Y, Lamed R. The cellulosomes: multienzyme machines for degradation of plant cell wall polysaccharides. *Annu Rev Microbiol.* 2004;58:521–54.
71. Bayer EA, Lamed R, White BA, Flint HJ. From cellulosomes to cellulosomes. *Chem Rec.* 2008;8:364–77.
72. Xu C, Huang R, Teng L, Jing X, Hu J, Cui G, Wang Y, Cui Q, Xu J. Cellulosome stoichiometry in *Clostridium cellulolyticum* is regulated by selective RNA processing and stabilization. *Nat Commun.* 2015;6:6900.
73. Balcázar JL, Blas ID, Ruiz-Zarzuela I, Cunningham D, Vendrell D, Múzquiz JL. The role of probiotics in aquaculture. *Vet Microbiol.* 2006;114:173–86.
74. Jabari L, Gannoun H, Cayol J-L, Hedi A, Sakamoto M, Falsen E, Ohkuma M, Hamdi M, Fauque G, Ollivier B, Fardeau M-L. *Macellibacteroides fermentans* gen. nov., sp. Nov., a member of the family *Porphyromonadaceae* isolated from an upflow anaerobic filter treating abattoir wastewaters. *Int J Syst Evol Microbiol.* 2012;62:2522–7.
75. Jiang Y, Caixia X, Yang G, Gong X, Chen X, Xu L, Bao B. Cellulase-producing bacteria of *Aeromonas* are dominant and indigenous in the gut of *Ctenopharyngodon idellus* (Valenciennes). *Aquac Res.* 2011;42:499–505.
76. Li H, Wu S, Wirth S, Hao Y, Wang W, Zou H, Li W, Wang G. Diversity and activity of cellulolytic bacteria, isolated from the gut contents of grass carp (*Ctenopharyngodon idellus*) (Valenciennes) fed on Sudan grass (*Sorghum sudanense*) or artificial feedstuffs. *Aquac Res.* 2016;47:153–64.
77. Li H, Zheng Z, Cong-xin X, Bo H, Chao-yuan W, Gang H. Isolation of cellulose—producing microbes from the intestine of grass carp (*Ctenopharyngodon idellus*). *Environ Biol Fishes.* 2009;86:131–5.
78. Bitterlich G. Digestive enzyme pattern of two stomachless filter feeders, silver carp, *Hypophthalmichthys molitrix* Val., and bighead carp, *Aristichthys nobilis* Rich. *J Fish Biol.* 1985;27:103–12.
79. Kolar CS, Chapman DC, Courtenay WR, Housel CM, Williams JD, Jennings DP. Bigheaded carps: a biological synopsis and environmental risk assessment. 2007.
80. Callejón-Leblic B, Selma-Royo M, Collado MC, Gómez-Ariza JL, Abril N, García-Barrera T. Untargeted gut metabolomics to delve the interplay between selenium supplementation and gut microbiota. *J Proteome Res.* 2022;21:758–67.
81. Wang C-L, Wang Z-Y, Song C-W, Luo S, Yuan X-Y, Huang Y-Y, Desouky HE. A comparative study on growth, muscle cellularity and flesh quality of farmed and imitative ecological farming loach, *Misgurnus anguillicaudatus*. *Aquaculture.* 2021;543:736933.
82. Barker HA. Amino acid degradation by anaerobic bacteria. *Annu Rev Biochem.* 1981;50:23–40.
83. Zhao J, Liu H, Michael A, Qiao S. Dietary protein and gut microbiome composition and function. *Curr Protein Pept Sci.* 2018;19:145–54.
84. Fan P, Song P, Li L, Huang C, Chen J, Yang W, Qiao S, Wu G, Zhang G, Ma X. Roles of biogenic amines in intestinal signaling. *Curr Protein Pept Sci.* 2017;18:532–40.
85. He L, Han M, Qiao S, He P, Li D, Li N, Ma X. Soybean antigen proteins and their intestinal sensitization activities. *Curr Protein Pept Sci.* 2015;16(7):613–21.
86. Hughes R, Magee EAM, Bingham S. Protein degradation in the large intestine: relevance to colorectal cancer. *Curr Issues Intest Microbiol.* 2000;1:51–8.
87. Sridharan GV, Choi K, Klemashevich C, Wu C, Prabakaran D, Pan LB, Steinmeyer S, Mueller C, Yousofshahi M, Alaniz RC, et al. Prediction and quantification of bioactive microbiota metabolites in the mouse gut. *Nat Commun.* 2014;5:5492.
88. Neis EP, Dejong CH, Rensen SS. The role of microbial amino acid metabolism in host metabolism. *Nutrients.* 2015;7:2930–46.
89. Metges CC, El-Khoury AE, Henneman L, Petzke KJ, Grant I, Bedri S, Pereira PP, Ajami AM, Fuller MF, Young VR. Availability of intestinal microbial lysine for whole body lysine homeostasis in human subjects. *Am J Physiol.* 1999;277:E597–607.

90. Giordano C, De Pascale C, Balestrieri C, Cittadini D, Crescenzi A. Incorporation of urea 15N in amino acids of patients with chronic renal failure on low nitrogen diet. *Am J Clin Nutr.* 1968;21:394–404.
91. Tanaka N, Kubo K, Shiraki K, Koishi H, Yoshimura H. A pilot study on protein metabolism in the Papua New Guinea highlanders. *J Nutr Sci Vitaminol.* 1980;26:247–59.
92. Metges CC, Petzke KJ, El-Khoury AE, Henneman L, Grant I, Bedri S, Regan MM, Fuller MF, Young VR. Incorporation of urea and ammonia nitrogen into ileal and fecal microbial proteins and plasma free amino acids in normal men and ileostomates. *Am J Clin Nutr.* 1999;70:1046–58.
93. Torrallardona D, Harris CI, Fuller MF. Pigs' gastrointestinal microflora provide them with essential amino acids. *J Nutr.* 2003;133:1127–31.
94. Torrallardona D, Harris CI, Fuller MF. Lysine synthesized by the gastrointestinal microflora of pigs is absorbed, mostly in the small intestine. *Am J Physiol-Endocrinol Metab.* 2003;284:E1177–80.
95. Wu G, Bazer FW, Davis TA, Jaeger LA, Johnson GA, Kim SW, Knabe DA, Meininger CJ, Spencer TE, Yin Y-L. Important roles for the arginine family of amino acids in swine nutrition and production. *Livest Sci.* 2007;112:8–22.
96. Li P, Mai K, Trushenski J, Wu G. New developments in fish amino acid nutrition: towards functional and environmentally oriented aquafeeds. *Amino Acids.* 2009;37:43–53.
97. Huang X-H, Zheng X, Chen Z-H, Zhang Y-Y, Du M, Dong X-P, Qin L, Zhu B-W. Fresh and grilled eel volatile fingerprinting by e-Nose, GC-O, GC-MS and GC × GC-QTOF combined with purge and trap and solvent-assisted flavor evaporation. *Food Res Int.* 2019;115:32–43.
98. Zhang Y, Venkatasamy C, Pan Z, Wang W. Recent developments on umami ingredients of edible mushrooms—a review. *Trends Food Sci Technol.* 2013;33:78–92.
99. Zhu W, Luan H, Bu Y, Li J, Li X, Zhang Y. Changes in taste substances during fermentation of fish sauce and the correlation with protease activity. *Food Res Int.* 2021;144: 110349.
100. Mouritsen OG, Khandelia H. Molecular mechanism of the allosteric enhancement of the umami taste sensation. *FEBS J.* 2012;279:3112–20.
101. Zhang L, Li Q, Lyu J, Kong C, Song S, Luo Y. The impact of stunning methods on stress conditions and quality of silver carp (*Hypophthalmichthys molitrix*) fillets stored at 4°C during 72h postmortem. *Food Chem.* 2017;216:130–7.

Publisher's Note

Springer Nature remains neutral with regard to jurisdictional claims in published maps and institutional affiliations.

Ready to submit your research? Choose BMC and benefit from:

- fast, convenient online submission
- thorough peer review by experienced researchers in your field
- rapid publication on acceptance
- support for research data, including large and complex data types
- gold Open Access which fosters wider collaboration and increased citations
- maximum visibility for your research: over 100M website views per year

At BMC, research is always in progress.

Learn more biomedcentral.com/submissions

